

Function and Characterization of Metal Oxide–Nafion Composite Membranes for Elevated-Temperature H₂/O₂ PEM Fuel Cells

Kevoork T. Adjemian,[†] Raymond Dominey,^{†,‡} Lakshmi Krishnan,[†] Hitoshi Ota,^{†,||}
Paul Majsztzik,[†] Tao Zhang,[†] Jonathan Mann,[†] Brent Kirby,[†] Louis Gatto,[†]
Melanie Velo-Simpson,[†] Jacklyn Leahy,[†] Supramanian Srinivasan,^{†,§} Jay B. Benziger,[⊥] and
Andrew B. Bocarsly^{*,†}

Department of Chemistry and Department of Chemical Engineering, Princeton University,
Princeton, New Jersey 08544, and Mitsubishi Chemical Group, Science and Technology Research Center,
Yokohama, Japan

Received August 9, 2005. Revised Manuscript Received February 14, 2006

Metal-oxide-recast Nafion composite membranes were studied for operation in hydrogen/oxygen proton-exchange membrane fuel cells (PEMFC) from 80 to 130 °C and at relative humidities ranging from 75 to 100%. Membranes of nominal 125 μm thickness were prepared by suspending a variety of metal oxide particles (SiO₂, TiO₂, Al₂O₃, and ZrO₂) in solubilized Nafion. The composite membranes were characterized using electrochemical, X-ray scattering, spectroscopic, mechanical, and thermal analysis techniques. Membrane characteristics were compared to fuel cell performance. These studies indicated a specific chemical interaction between polymer sulfonate groups and the metal oxide surface for systems that provide a good elevated-temperature (i.e., fuel-cell operation above 120 °C) performance. Composite systems that incorporate either a TiO₂ or a SiO₂ phase produced superior elevated-temperature, low-humidity behavior compared to that of a simple Nafion-based fuel cell. Improved temperature tolerance permits the introduction of at least 500 ppm CO contaminant in the H₂ fuel stream without cell failure, in contrast to standard Nafion-based cells, which fail below 50 ppm of carbon monoxide.

Introduction

To solve both the carbon monoxide poisoning and the water thermal-management problems associated with current hydrogen–oxygen proton-exchange membrane (PEM) fuel-cell technology, we need to modify present state-of-the-art perfluorosulfonic acid (PFSA) membranes, such as Nafion, in order for them to remain conductive at operating temperatures above ~90 °C. This paper evaluates the water-retention capabilities of Nafion at 130 °C in a PEM fuel cell (PEMFC) and how it is impacted by the incorporation of various metal oxide particles into the PFSA structure to form a composite membrane. The metal oxide particles studied include silica, titania, alumina, and zirconia.

Previous efforts^{1,2} to enhance the water retention of Nafion and related membranes by incorporating metal oxide particles such as SiO₂ produced promising results. Antonucci et al.¹ studied a silica composite membrane in a direct methanol fuel cell, which produced 600 mA cm⁻² at a potential of 0.4 V. Antonucci attributed the enhanced performance of the composite membrane to the hygroscopic properties of silica. Watanabe et al.² investigated silica- and titania-impregnated

Nafion composite membranes in H₂/O₂ proton-exchange membrane fuel cells operating at 100 °C with minimal external humidification. They reported that the silica particles were superior to titania particles in terms of water-retention qualities within the Nafion membrane and attributed this effect to the higher water sorption properties of silica. Mauritz et al.³ proposed a sol–gel approach of adding silica to a Nafion membrane that might provide superior performance to particles, because the sol–gel produced silica is homogeneously dispersed on the angstrom scale versus submicrometer-length scales for the particle composites.

In this paper, a different model is put forward for the beneficial effects of metal oxide particles on high-temperature PEMFC operations. It is suggested that improved cell behavior is not related to water retention or the acidity properties of the metal oxide component but rather to the effect of the metal oxide particle on the temperature-dependent structure of the polymer matrix. Special attention is given to the physicochemical characteristics of the various simple metal oxide composites under investigation. In particular, an understanding of the interfacial chemistry that occurs between the metal oxide particles and the Nafion membrane is emphasized, along with a consideration of how this interface affects elevated-temperature fuel-cell dynamics.

Experimental Section

Preparation of Composite Membranes. Metal oxide particles were purchased either from Alfa-Aesar, Aldrich, GFS Chemicals,

* To whom correspondence should be addressed. Phone: (609) 258 3888. Fax: (609) 258 2383. E-mail: bocarsly@princeton.edu.

[†] Department of Chemistry, Princeton University.

[‡] Present address: Department of Chemistry, University of Richmond.

^{||} Mitsubishi Chemical Group Science and Technology Research Center.

[§] Presented posthumously.

[⊥] Department of Chemical Engineering, Princeton University.

(1) Antonucci, P. L.; Arico, A. S.; Creti, P.; Ramunni, E.; Antonucci, V. *Solid State Ionics* **1999**, *125* (1–4), 431–437.

(2) Watanabe, M.; Uchida, H.; Seki, Y.; Emori, M.; Stonehart, P. *J. Electrochem. Soc.* **1996**, *143* (12), 3847–3852.

(3) Deng, Q.; Moore, R. B.; Mauritz, K. A. *Chem. Mater.* **1995**, *7* (12), 2259–2268.

Table 1. Metal Oxides Physical Composition^a

| metal oxide | size | surface area (m ² /g) |
|---|------------|----------------------------------|
| SiO ₂ (AA) | 0.2–0.3 μm | 90 |
| SiO ₂ (DH) | 20 nm | 90 |
| Al ₂ O ₃ (AA) | 1 μm | 6–8 |
| Al ₂ O ₃ (AA) | 25 μm | 6 |
| Al ₂ O ₃ (DH) | 13 nm | 100 |
| TiO ₂ (AA) | 1–2 μm | 3–6 |
| TiO ₂ (AA-acid treated/ degreased) | 1–2 μm | 3–6 |
| TiO ₂ (AA)-silylated | 1–2 μm | 3–6 |
| TiO ₂ (DH) | 21 nm | 50 |
| ZrO ₂ (AA) | 7.5 μm | |
| ZrO ₂ (GFS) | 44 μm | |
| ZrO ₂ (Aldrich) | 1.5 μm | 0.38 |

^a AA = Alfa-Aesar, DH = Degussa-Huls.

or Degussa-Huls, as reported in Table 1, and were used as received. Composite membranes were prepared by mixing 5% commercial Nafion 1100 solution (Ion Power Inc.) with double its volume of isopropyl alcohol and 3% (by weight of dry Nafion) metal oxide. This suspension was stirred at room temperature for 3 h and then dried at 70 °C overnight. Once the solvent removal was complete, the product film was heat-treated at 145 °C for 20 min. The high-temperature annealing process resulted in a brown membrane due to residual organics.

Crude membranes were post-treated as follows: (i) refluxing in boiling 3% H₂O₂ (by volume) for 1 h to oxidize the organic impurities; (ii) soaking in boiling deionized H₂O for 1 h; (iii) refluxing in boiling 0.5 M H₂SO₄ for 1 h to remove any metallic impurities and ensure complete protonation of the Nafion; and (iv) soaking in boiling deionized H₂O for 2 h to remove excess acid.

The cleaned composite membranes were cloudy in appearance. The titania composites provided an opaque white membrane. Metal oxide loading was limited to 3 wt %, as higher loadings produced a material that was subject to cracking.

In an additional set of experiments, TiO₂ particles were also treated by the following methods before being added to the Nafion solution: (i) Particles were treated with acid by mixing them in concentrated H₂SO₄ (95–98%, Fisher) for 6–8 h followed by filtering and rinsing several times with deionized water. Samples were then dried overnight at 90 °C. (ii) Degreasing by mixing and filtering the particles in various solvents, including (in order of increasing hydrophilicity) toluene, hexanes, isopropyl alcohol, and water, and drying them overnight at 90 °C. (iii) Acid-treated TiO₂ was also reacted with trichloromethylsilane (98% Aldrich) under N₂ in hexane for 8 h to silylate the surface hydroxyl groups. The particles were then filtered, rinsed, and dried overnight at 90 °C.

Characterization of Composite Membranes. Electron microprobe (CAMECA SX-50) analysis was used to analyze the distribution of the metal oxide over the cross section of the composite membranes.

Fluorescence experiments to probe the chemical environment within the membranes using pyrene (99%, Aldrich) were performed on a Fluorolog spectrometer. The emission spectra were obtained using an excitation wavelength of 333 nm with 1.0 nm slit widths for both excitation and emission monochromators. Samples for the fluorescence experiments⁴ were prepared by making the various composite membranes as described earlier in this section followed by drying the membranes at 90 °C overnight. The membranes were then soaked in a 0.01 M pyrene/methanol solution for 10 h, wiped to remove externally adherent solution, and then dried again at 90 °C overnight.

The equivalent weight of the composite membranes was determined by an acid–base titration. The membranes were dried under vacuum at 80 °C for 24 h followed by soaking in 1.0 M NaCl (EM Science, 99%) overnight. The salt solution (25 mL) was titrated with 0.01 M NaOH (Alfa-Aesar, standardized) with phenol red indicator. The volume of NaOH consumed and the dry weight of the membranes were used to calculate the equivalent weight. The titration was repeated for concordant values.

The glass-transition temperature of the metal oxide composite membranes was obtained by dynamic mechanical analysis (DMA) using an ARES strain rheometer (Rheometric Scientific) equipped with a high-resolution actuator for low-strain measurements. DMA experiments were run using a 5 °C/min heating rate, 1 Hz frequency, and 0.03% strain.

The hydrophilicity of membrane surfaces was assessed via contact angle using a Tante contact angle meter. Measurements were made by first submerging the membrane sample in room temperature DI water for several minutes, spreading the saturated membrane flat on a clean glass microscope slide, and finally removing excess surface water by wiping with a Kimwipe. The contact angle was then immediately measured.

Small-angle X-ray scattering (SAXS) was performed using a Philips XRG-3000 sealed-tube X-ray source, which produces both Cu Kα and Cu Kβ X-rays. The scattered X-rays were detected using a Kratky camera (Anton-Paar, 54 cm) equipped with a multichannel detector (Braun OED-50M). Data collection was performed under helium to minimize outside scattering and lasted 10 minutes. The membrane samples were equilibrated with liquid water for various times, and measurements were taken as a function of water content.

Temperature-programmed decomposition of membrane materials was carried out using thermal gravimetric mass spectroscopy using a Seiko EXSTAR 6000 TG-DTA interfaced to an Agilent 6890N GC/MS. The pyrolysis temperature was programmed to increase from 25 to 500 °C at a rate of 10 °C/min under a helium flow of 60 mL/min. The gaseous decomposition products were introduced directly into the MS unit via a gas-transfer tube with a deactivated fused silica capillary. The transfer lines were maintained at 200 °C. The MS interface temperature was set at 250 °C. The MS system was maintained at about 1 × 10⁻⁶ Torr.

Preparation of Electrodes and Fuel-Cell Testing. Commercial Pt/C electrodes (ETEK Inc.) with a Pt loading of 0.4 mg/cm² were impregnated with 0.6 mg/cm² of Nafion (Ion-Power, 5% solution). The active electrode area was 5 cm². Membrane–electrode assemblies (MEA) were prepared by heating an electrode/membrane/electrode sandwich from room temperature to 140 °C with no applied pressure. Proper interfacial adhesion in the MEA was achieved by pressing the sandwich in a Carver hot press at 140 °C with 250 psi for 90 s. Subsequently, the sandwich was cooled on the benchtop before being assembled in a single-cell testing unit. The single cell was then installed in the fuel-cell test station (Globetech Inc., GT-1000). The test station was equipped for the temperature-controlled humidification of the reactant gases (H₂, O₂, and N₂) and independent temperature control of the single cell. Flow rates of the gases were regulated using mass-flow controllers, and the total pressure of the gases was controlled using back-pressure regulators.

For the performance evaluation of the PEMFC, we fed the single cell with humidified H₂ and O₂ at atmospheric pressure (reactant gas and water vapor pressure equal to 1 atm). The cell was allowed to run for 8 h at 50 °C with the anode and cathode humidification bottles at 70 °C at a potential ~0.9 V to allow oxidation of any organic impurities present. The temperatures of the humidifiers and the single cell were raised to 90, 80, and 90 °C (anode humidification temperature, cell temperature, and cathode humidification

(4) Deng, Q.; Hu, Y.; Moore, R. B.; McCormick, C. L.; Mauritz, K. A. *Chem. Mater.* **1997**, *9* (1), 36–44.

temperature, respectively). The cathode was then purged with nitrogen, and cyclic voltammograms were recorded at 100 mV s^{-1} between 0.1 and 1 V vs RHE for 1 h to determine the electrochemically active surface area of the electrodes. The single cell was then stabilized at a potential of $\sim 0.35 \text{ V}$ to ensure complete hydration of the membrane with the water produced at the cathode prior to the high-temperature measurements.

Cell potential vs current density measurements were performed under the desired conditions of temperature and pressure in the PEMFC. Identical procedures were followed for all of the membranes. All PEMFC experiments were carried out at cell temperatures of 80 and 130 °C, with the total pressure (reactant gas plus water vapor pressure) at 1 and 3 atm, respectively. Initially, data were collected at 100% relative humidity, and the temperature of the humidifier bottles was decreased to record performance data at lower relative humidities. In all cases, a flow rate of 40 mL/min was employed. It is important to note that the relative humidity values reported are calculated values on the basis of the vapor pressure of water at 130 °C (cell temperature) and the respective anode and cathode bottle humidification temperatures. For instance, when the cell temperature is 130 °C (vapor pressure of water at 130 °C is 2.67 atm) and the temperature of the anode and cathode humidification bottles is also 130 °C, the relative humidity in the cell is 100%. Consequently, the temperature of the humidifier bottles at 128 °C (vapor pressure of water at 128 °C is 2.51 atm) with the cell maintained at 130 °C provides a 96% relative humidity in the cell and so on. The temperatures of the humidifier bottles were decreased to 128, 124, and 122 °C, with the cell temperature at 130 °C, to attain 96, 88, and 75% relative humidity, respectively. Calibration experiments in which the output of the cell was evaluated using a humidity sensor indicated that the calculated values were a good indication of the actual cell humidity. A 1 h period was used between changes in systems temperatures and collection of current–voltage data to permit temperature and potential stabilization before data acquisition.

The carbon monoxide experiments were carried out at 130 °C under saturation and 75% RH conditions. The single cell was purged with a hydrogen stream containing 100 or 500 ppm of CO at a constant load until the potential remained steady, and polarization curves were recorded. The H_2/CO purge typically lasted 4 h before data collection. For some of the carbon monoxide experiments, Pt/Ru/C (1:1 Pt:Ru ratio) electrodes (ETEK Inc.) with a Pt loading of 0.4 mg/cm^2 were used at the anode and were prepared in the same manner as the Pt/C electrodes.

Results and Discussion

Chemical and Electrochemical Characterization of Composite Membrane Materials. The electron microprobe data in Figure 1 shows a homogeneous and uniform distribution of Si and O across the SiO_2 –Nafion composite membrane cross section on a scale of $20 \mu\text{m}$, synthesized by dispersion of $2 \mu\text{m}$ SiO_2 particles from Alfa-Aesar in Nafion solution. All composite membranes tested showed identical homogeneity.

Cyclic voltammograms for the cathode with the unmodified recast Nafion and all composite membranes were obtained. By integrating the oxidation peak at 0.1 V vs RHE and assuming a coulombic charge of $220 \mu\text{C cm}^{-2}$ for the oxidation of atomic hydrogen on a smooth platinum surface, we obtained an average roughness factor of $135 \text{ cm}^2 \text{ cm}^{-2} \pm 15 \text{ cm}^2 \text{ cm}^{-2}$ for all composite membranes. With consistent roughness factors, no effect on the activity of Pt electrocatalyst by the metal oxide was seen.

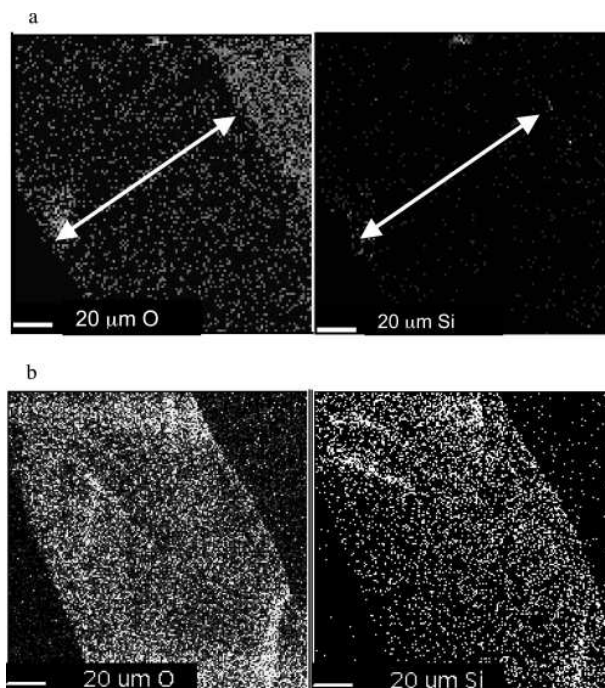


Figure 1. EPMA data obtained for freeze-fractured cross sections of (a) a recast Nafion membrane and (b) a SiO_2 recast composite membrane showing Si (righthand side) and O (lefthand side) distribution maps within the Nafion structure. The arrow indicates the thickness of the plain Nafion membrane. The recast membrane was synthesized by dispersion of $2 \mu\text{m}$ SiO_2 particles (3 wt %) from Alfa-Aesar in Nafion recasting solution. The intensity of the white dots qualitatively indicates the amount of the indicated element present.

A main objective of this study was to determine which chemical attributes of the composite membranes improve water management at elevated temperature and thereby improve PEMFC performance. The parameters of interest included the type of metal oxide, surface area, size, and surface chemical modification of the metal oxide. The primary tool for carrying out this analysis was a comparison of the current–voltage response of the cell as a function of membrane chemical characteristics and cell humidity/temperature. In the present study, the operating temperature of the gas humidifiers was limited to 130 °C. Under this condition, the total pressure was increased to 3 atm, because the vapor pressure of water at this temperature is 2.6 atm.

The cell potential (E) versus current density (i) data were analyzed by fitting the PEMFC data points to eq 1

$$E = E_0 - b \log i - Ri \quad (1)$$

where E and i are the measured cell potential and current. E_0 is defined by eq 2, b is the Tafel slope, and R accounts for the linear variation of overpotential with current density primarily due to ohmic resistance. The exchange-current density (i_0) of the oxygen-reduction reaction was calculated by using eq 2

$$E_0 = E_r + b \log i_0 \quad (2)$$

where E_r is the thermodynamically reversible cell potential.

The electrode kinetic parameters derived from eqs 1 and 2 as a function of metal oxide employed are presented in Tables 2 and 3.

Table 2. Electrode Kinetic Parameters of SiO₂ and TiO₂ Composite Membranes at 130 °C, 30 psig, and Various Calculated Relative Humidities in PEMFCs with H₂/O₂ Reactant Gases^a

| RH (%) | E ₀ (mV) | b (mV/decade) | R (ohm cm ²) | cell potential at 600 mA/cm ² (mV) |
|------------------------------|---------------------|---------------|--------------------------|---|
| Plain Recast | | | | |
| 100 | 961 | 65 | 0.26 | 632 |
| 94 | 960 | 59 | 0.52 | 491 |
| 88 | 935 | 50 | 0.65 | 435 |
| 75 | 940 | 54 | 0.9 | |
| SiO ₂ (AA) | | | | |
| 100 | 950 | 60 | 0.23 | 648 |
| 94 | 950 | 60 | 0.27 | 624 |
| 88 | 957 | 67 | 0.27 | 611 |
| 75 | 975 | 82 | 0.29 | 573 |
| SiO ₂ (DH) | | | | |
| ~100 | 954 | 54 | 0.25 | 659 |
| 94 | 954 | 53 | 0.27 | 648 |
| 88 | 955 | 54 | 0.29 | 636 |
| 75 | 967 | 65 | 0.33 | 587 |
| TiO ₂ (AA) | | | | |
| ~100 | 948 | 49 | 0.41 | 580 |
| 94 | 965 | 57 | 0.42 | 564 |
| 88 | 974 | 65 | 0.45 | 526 |
| 75 | 976 | 68 | 0.58 | 424 |
| TiO ₂ (DH) | | | | |
| ~100 | 960 | 54 | 0.25 | 662 |
| 94 | 959 | 53 | 0.28 | 648 |
| 88 | 959 | 54 | 0.31 | 633 |
| 75 | 980 | 70 | 0.35 | 582 |
| TiO ₂ (degreased) | | | | |
| 75 | 908 | 65 | 0.33 | 590 |
| TiO ₂ (silylated) | | | | |
| 75 | 897 | 77 | 0.36 | 400 |

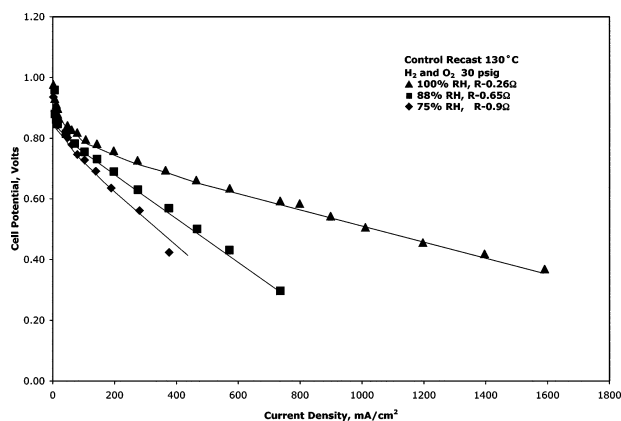
^a AA = Alfa-Aesar, DH = Degussa-Huls.**Figure 2.** Current–voltage profiles for a membrane electrode assembly (MEA) utilizing a Nafion recast membrane at various relative humidities with a cell maintained at 130 °C, 30 psig of H₂/O₂ reactant gases. Relative humidity in the cell was calculated from the saturation vapor pressure of water at the cell, anode, and cathode humidifier temperatures.

Figure 2 shows the polarization curve of a recast Nafion membrane at a cell temperature of 130 °C and different relative humidities. The *R* value, as defined by eq 1, increased 3-fold (Table 2) upon decreasing the relative humidity in the cell to 75%. Below 75% relative humidity, the cell exhibited unstable current and voltage values. The observed degradation in the performance can be attributed to the loss of water from the membrane. Water loss is anticipated to have two negative impacts on cell performance: membrane proton conductivity is decreased and shrinkage of the

Table 3. Electrode Kinetic Parameters of Al₂O₃ and ZrO₂ Composite Membranes at 130 °C, 30 psig, and Various Calculated Relative Humidities in PEMFCs with H₂/O₂ Reactant Gases^a

| RH (%) | E ₀ (mV) | b (mV/decade) | R (ohm cm ²) | cell potential at 600 mA/cm ² (mV) |
|---|---------------------|---------------|--------------------------|---|
| Plain Recast | | | | |
| 100 | 961 | 65 | 0.26 | 632 |
| 94 | 960 | 59 | 0.52 | 491 |
| 88 | 935 | 50 | 0.65 | 435 |
| 75 | 940 | 54 | 0.9 | |
| Al ₂ O ₃ , 1 μm (AA) | | | | |
| 100 | 946 | 52 | 0.32 | 625 |
| 94 | 960 | 74 | 0.48 | 462 |
| 88 | 968 | 77 | 0.55 | 426 |
| 75 | 970 | 84 | 0.79 | 406 |
| Al ₂ O ₃ , 25 μm (AA) | | | | |
| 100 | 953 | 45 | 0.29 | 664 |
| 94 | 960 | 69 | 0.4 | 538 |
| 88 | 954 | 61 | 0.54 | 458 |
| 75 | 970 | 57 | 0.7 | 344 |
| ZrO ₂ 6 μm (AA) | | | | |
| 100 | 958 | 51 | 0.29 | 645 |
| 94 | 964 | 57 | 0.32 | 617 |
| 88 | 962 | 54 | 0.4 | 575 |
| 75 | 965 | 72 | 0.54 | 458 |
| ZrO ₂ 1 μm (AA) | | | | |
| 100 | 960 | 55 | 0.32 | 620 |
| 94 | 970 | 62 | 0.41 | 568 |
| 88 | 953 | 60 | 0.58 | 449 |
| 75 | 970 | 83 | 0.7 | 400 |
| ZrO ₂ (Aldrich) | | | | |
| ~100 | 944 | 57 | 0.25 | 646 |
| 78 | 964 | 64 | 0.62 | 442 |
| ZrO ₂ (GFS) | | | | |
| ~100 | 939 | 52 | 0.57 | 454 |
| 78 | 986 | 105 | 0.85 | |

^a AA = Alfa-Aesar.

membrane is expected to degrade the membrane–electro-catalyst interface.

Fuel-Cell Performance of SiO₂ and TiO₂ Composites.

The physical characteristics of the metal oxides used to prepare the composite membranes are reported in Table 1. At 100% RH, there was no significant difference in fuel-cell performance due to metal oxide impregnation, with the exception of Alfa-Aesar titania-impregnated membranes, which showed an increased *R* value (see Table 2 and Figure 3a). This variation is not intrinsic to TiO₂-impregnated membranes, because the use of Degussa-Huls titania does not produce an unusually high cell resistivity, and its effect will be considered later in this paper. When the humidifier bottle temperatures were reduced such that the RH was 88% in the cell (Figure 3b), SiO₂ and TiO₂ composite membranes yielded current–voltage characteristics that outperformed control recast Nafion membranes, as shown in Figure 3b. The trend from lowest resistance and higher cell potential at a given current density at 88% relative humidity is as follows

$$\text{DH SiO}_2 \approx \text{AA SiO}_2 \approx \text{DH TiO}_2 >$$

$$\text{AA TiO}_2 \gg \text{plain recast}$$

where DH and AA represent Degussa-Huls and Alfa-Aesar metal oxides, respectively. The performance of the silica and titania composites at 130 °C and 75% RH is reported in Figure 3c, in which it is observed that the output parameters

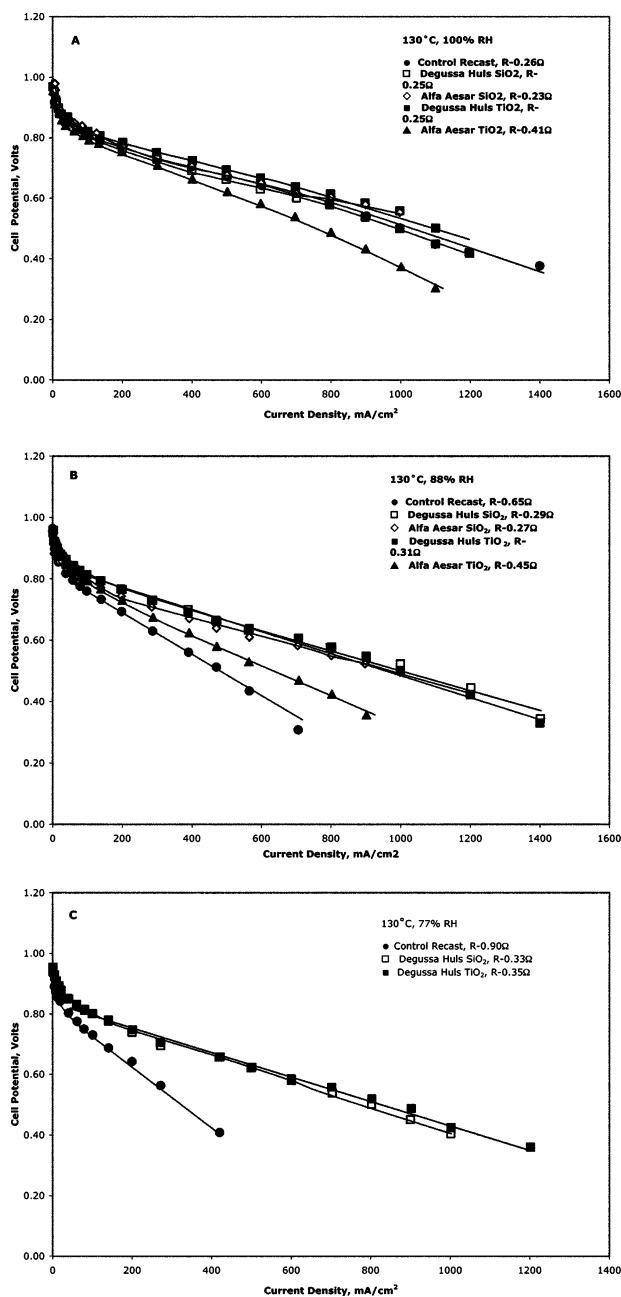


Figure 3. Current–voltage profiles for MEAs containing SiO_2 and TiO_2 composite membranes with (a) 100% RH, (b) 88% RH, and (c) 75% RH. In all cases, the cell temperature was maintained at 130 °C with a gas pressure of 30 psig. The physical characteristics of the metal oxide particles are reported in Table 1. Relative humidity in the cell was calculated from the saturation vapor pressure of water at the cell, anode, and cathode humidifier temperatures.

of the recast Nafion-based cell continue to deteriorate ($0.9 \Omega \text{ cm}^2$ cell resistivity), but the composite membrane systems provide essentially relative humidity invariant of the cell conductivity. Thus, under saturation conditions, the recast Nafion and Nafion–metal oxide composite membranes yield similar proton conductivities; once the vapor phase water partial pressure is dropped below its saturation value, the composite MEA exhibits superior proton conductivity. This suggests a structural change in the composite membrane that enhances the water content when compared to a recast Nafion

at elevated temperatures and reduced relative humidity. This finding is consistent with our prior reports^{5,6} that demonstrate that incorporation of silicon oxide via sol–gel processing improves the water management characteristics of a Nafion membrane in a PEMFC operating above 100°C.

Metal Oxide–Nafion Interfacial Interactions. Although the performance of the silica composite was independent of the manufacturing source and physical properties (i.e., particle size, surface area, etc.), the observed cell resistance of MEAs containing titania composites made from Alfa-Aesar titania were almost twice as resistive as membranes that incorporated Degussa-Huls titania. Additionally, the Alfa-Aesar titania produced a composite membrane that underperformed the pure recast Nafion membrane at 100% RH (see Figure 3a), although some advantage was observed when this membrane was compared with a pure recast Nafion membrane under reduced humidity conditions (Figure 3b,c). Given that both titania suppliers report similar chemical composition and particle physical properties, this observation suggests that particle-surface chemistry (or properties) may play a key role in developing a pragmatic, polymer–inorganic, composite, high-temperature membrane.

One possible explanation for the observed difference is the presence of a contaminating interfacial layer on one of the titania surfaces. Such a surface layer could be either detrimental or advantageous, depending on how it interacts with the surrounding Nafion matrix. To probe this hypothesis, we processed titania samples from Alfa-Aesar, which provided a poor membrane response, using two separate treatments (see the Experimental Section). In one case, a standard degreasing set of solvents was employed, starting with toluene and ending with 2-propanol and water. Alternately, the samples were carried through an acidification step (using concentrated sulfuric acid) aimed at increasing the surface hydroxyl content. (This latter process is expected to incidentally remove a hypothetical organic surface layer, although that is not the primary goal of this process.) Titania treated in either manner produced a membrane that provided improved PEMFC performance (resistance value of $0.33 \Omega \text{ cm}^2$ vs $0.58 \Omega \text{ cm}^2$ for the untreated particles at 75% RH), suggesting surface contamination of the titania particles from Alfa-Aesar and that such surface contamination was detrimental to membrane performance. The electrode kinetic parameters for the treated particle-membrane-based cells under 75% RH are reported in Table 2. Membranes utilizing titania particles from Degussa-Huls gave the same response in a PEMFC, regardless of whether the particles were used as received, treated with acid, or solvent-degreased.

Further support for the presence of a detrimental organic-based surface layer was obtained by reacting as-received titania particles from Degussa-Huls and solvent-treated titania particles from Alfa-Aesar with trichloromethylsilane in hexane, as described in the Experimental Section. This process silylates the surface via reaction with surface hydroxyl groups and forms a layer of surface-attached

(5) Adjemian, K. T.; Lee, S. J.; Srinivasan, S.; Benziger, J.; Bocarsly, A. B. *J. Electrochem. Soc.* **2002**, *149* (3), A256–A261.

(6) Adjemian, K. T.; Srinivasan, S.; Benziger, J.; Bocarsly, A. B. *J. Power Sources* **2002**, *109* (2), 356–364.

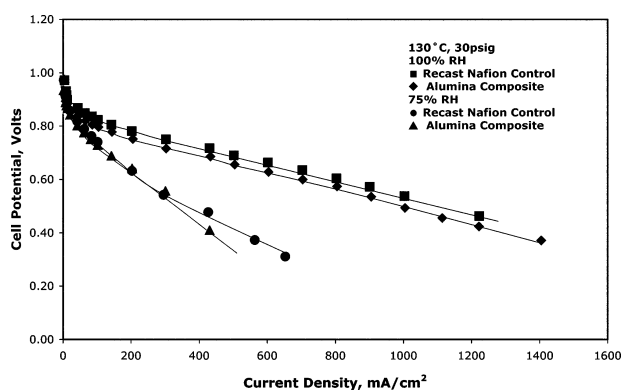


Figure 4. Current–voltage profiles for a MEA containing an alumina composite membrane; cell temperature was 130 °C, relative humidity was 100 and 75% and 30 psig of H₂/O₂ reactant gases. Relative humidity in the cell was calculated from the saturation vapor pressure of water at the cell, anode, and cathode humidifier temperatures.

polymerized polysiloxane. Membranes and MEAs fabricated from the silylated titania particles showed increased cell resistance and degraded current–voltage characteristics (see Table 2). Although this observation is given as support for the negative impact of an interfacial organic layer, it could also indicate that surface hydroxyl groups are the reactive sites needed to provide the requisite interaction between the titania particles and the Nafion polymer. This interpretation is consistent with the observation that acid treatment, a process that induces surface hydroxyl functionalities, improves the membrane response. However, it is not consistent with the observation that a degreasing process leads to improved membrane response.

X-ray powder diffraction of the Alfa-Aesar and Degussa-Huls titania products indicates that the former product is a pure rutile phase, whereas the latter material is a mixed phase containing ~70% rutile and ~30% anatase. It has been noted that the anatase phase is primarily composed of the (1,0,1) crystal face.⁷ This phase is rich in a coordinately unsaturated Ti(IV) site, which may represent a site of ligation with polymer sulfonate groups, as discussed later. However, on the basis of the data reported above, the primary difference between the two titania samples employed must be the purity of the titania surface. In any event, the data presented here strongly point to an interfacial interaction as central to the improved behavior of the composite membranes.

Performance of Alumina and Zirconia Composites. To further probe the potential role of a chemical interaction between the metal oxide interface and the Nafion sulfonate groups, we constructed composite membranes containing alumina (Al₂O₃) particles. This material was selected because it is significantly more chemically reactive than titania. As is observed in Figure 4, even at 100% RH (130 °C) where pure recast Nafion membranes and titania composites show identical behavior, a Degussa-Huls alumina composite is detrimental to the PEM fuel-cell performance. The types of surface processing discussed in the prior section did not yield improved materials. From the electrode kinetic parameter values reported in Table 2, it can be seen that the alumina composites from Alfa-Aesar showed a performance that is at best comparable to the unmodified recast membrane at 75% relative humidity. One possible reason for the observed

decrease in performance is the potential release of Al³⁺ ions into the membrane. This process is expected to be facilitated by the acidic pK_a of Nafion. To test this hypothesis, we soaked samples of alumina from Degussa-Huls and Alfa-Aesar in 0.5 M H₂SO₄ for 1 h. The solutions were then partially neutralized with sodium carbonate to pH ~5.5, and the colorimetric Al³⁺ indicator Alizarin S was added. Both solutions were observed to turn red, indicating the presence of a substantial concentration of solubilized aluminum.⁸ The release of Al³⁺ into the Nafion matrix will either displace a portion of the mobile protons from sulfonate sites or crosslink sulfonate sites, changing the local polymer morphology and potentially making proton sites inaccessible for ion-exchange purposes. Titration of metal-oxide-incorporated membranes reported in Table 3 does not provide evidence of proton consumption upon impregnation of the alumina. Therefore, the observed membrane response in the presence of alumina appears to be related to restricted proton conductivity, likely associated with an Al³⁺-induced change in the Nafion microstructure.

To gain more insight into the alumina composite, we also synthesized membranes containing a zirconia component. As can be seen from the electrochemical parameters presented in Table 2, these systems behaved in a manner very similar to the that of alumina-based composites, generally producing high-resistance cells that were not tolerant of low-humidity conditions. Like alumina, these composites did not consume excessive protons (see Table 3). However, the oxophilic nature of zirconium is expected to lead to the production of zirconium oxysulfate in the acidic Nafion environment, perturbing a fraction of the sulfonate sites. Similar to alumina, this type of reactivity is expected to modify the membrane topology, potentially limiting proton diffusion.

Physical Characterization of Composite Membranes. Pyrene as a Probe of the Hydrophilicity of the Composite. To evaluate the impact of composite formation on the hydrophilicity of the Nafion membranes and to determine the location of the metal oxide particles within the membrane matrix, we observed the fluorescence behavior of a pyrene probe. Pyrene has a monomer emission with a resolved vibronic structure that is sensitive to the polarity of its molecular environment.^{9–11} The emission spectrum of pyrene consists of five characteristic peaks. The ratio of the intensity of peak 3 (383 nm) to the intensity of peak 1 (372 nm) (*I*₃:*I*₁) decreases with an increase in environmental polarity (hydrophilicity) around the excited-state pyrene molecule. Examples of solvent media illustrating the influence of polarity show *I*₃:*I*₁ values ranging from 0.54 for water (intense polar solvent) to 2.00 in a fluorocarbon medium (extremely nonpolar solvent).¹⁰

Figure 5 shows the emission spectra of pyrene in Nafion and two metal oxide–Nafion composite membranes (Al₂O₃

- (7) Lazzeri, M.; Vittadini, A.; Selloni, A. *Phys. Rev. B* **2001**, 6315.
- (8) Snell, F. D. *Colorimetric Analysis*; Von Norstrand Co.: New York, 1921.
- (9) Dong, D. C.; Winnik, M. A. *Photochem. Photobiol.* **1982**, 35 (1), 17–21.
- (10) Kalyanasundaram, K.; Thomas, J. K. *J. Am. Chem. Soc.* **1977**, 99 (7), 2039–2044.
- (11) Kaufman, V. R.; Avnir, D. *Langmuir* **1986**, 2 (6), 717–722.

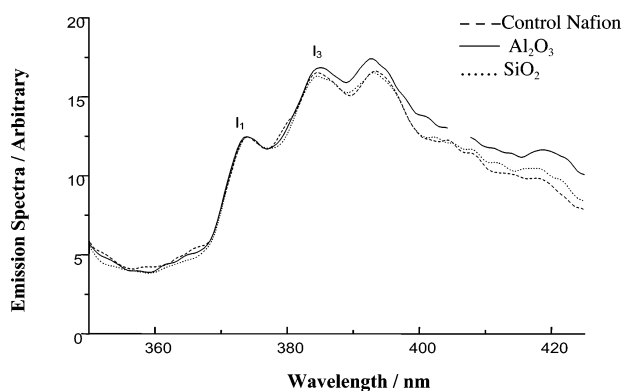


Figure 5. Fluorescence experiments of control and composite Nafion membranes. Spectra normalized to the I_1 peak of plain Nafion.

Table 4. $I_3:I_1$ Ratio and Proton Concentration on the Basis of Titration of Composite Membranes

| metal oxide | $I_3:I_1$ | % protons consumed |
|--|-----------|--------------------|
| SiO ₂ (AA) | 1.29 | 5 |
| SiO ₂ (DH) | 1.35 | 3 |
| Al ₂ O ₃ (AA) | 1.35 | 4 |
| Al ₂ O ₃ (DH) | 1.36 | 3 |
| TiO ₂ (AA) | 1.36 | |
| TiO ₂ (AA) (acid treated/degreased) | 1.15 | 2 |
| TiO ₂ (AA)-silylated | 1.33 | |
| TiO ₂ (DH) | 1.21 | <1 |
| ZrO ₂ (AA, Aldrich) | | <1 |
| control Nafion | 1.34 | 0 |

AA-Alfa-Aesar, DH-Degussa-Huls

and SiO₂). All spectra were normalized to the I_1 peak. The observed intensity ratios for the other composite membrane systems are reported in Table 4. A comparison of $I_3:I_1$ ratios to the cell resistance observed for the associated (pyrene free) membrane, on the basis of the slope of the linear region of the $i-V$ curve, presents a clear trend between the two measurements (Tables 2–4). On the basis of the fact that the emission ratio is dependent on the metal oxide employed, we can conclude that the pyrene is localized at the metal oxide–Nafion interface. Given the self-organization of Nafion into hydrophilic regions containing the sulfonate moiety and hydrophobic regions containing the CF₂ polymer backbone, it also follows that the metal oxide particles are localized in the hydrophilic domains. If this were not the case, the pyrene intensity ratio should be invariant. Finally, it can be seen from Tables 2–4 that as the $I_3:I_1$ ratio decreases (increased hydrophilicity within the Nafion composite) the resistance value at 130 °C also decreases. That is, the presence of the metal oxide at 130 °C improves the hydrophilicity of the membrane and thereby the MEA performance. The more polar the environment between the metal oxide and the Nafion membrane, the better the composite membrane will perform in a PEMFC above 100 °C in an under humidified environment. Given that thermal gravimetric analyses of recast membranes, with and without a metal oxide component (independent of the metal oxide employed), show no significant difference in the quantity of water present or the temperature at which water is desorbed from the membrane, it cannot be concluded that the observed changes in hydrophilicity are associated with the retention of water by the metal oxide particles or at the metal oxide–polymer interface.

Table 5. Variation in Membrane-Surface Hydrophilicity as Monitored by Contact-Angle Measurements on Fully Hydrated Membranes

| sample | measured contact angle (deg) |
|--|------------------------------|
| Teflon | 112 |
| extruded Nafion (115 and 117) | 75–80 |
| recast Nafion (125 μ m membrane thickness) | 75–87 |
| composite membrane (3 wt % DH TiO ₂ , 125 μ m membrane thickness) | 74–84 |
| composite membrane (3 wt % AA TiO ₂ , 125 μ m membrane thickness) | 75–86 |

Contact-Angle Measurements as a Measure of Membrane Bulk Hydrophilicity. The impact of the metal oxide phase on the bulk hydrophilicity of composite TiO₂ membranes was assessed using contact-angle measurements on fully hydrated membranes. Membrane samples were cleaned and acidified prior to being equilibrated with water, using the same procedures utilized to prepare membranes for MEAs. As seen by the data presented in Table 5, recast membranes, independent of composition, were observed to present a more hydrophobic (Teflonic) surface than extruded materials. This is consistent with the model in which the sulfonate groups self-assemble in the solution phase of a recasting solution while the Teflonic polymer backbone orients on the hydrophobic (i.e., air) side of an aqueous–air interface. However, no significant difference was observed for recast membranes vs composite membranes made from either DH TiO₂ or AA TiO₂. Given that only the DH TiO₂ membrane provides a superior high-temperature, low-humidity fuel-cell performance, a change in the bulk hydrophilicity of the membrane upon addition of TiO₂ is ruled out as the source of the observed enhancement in fuel-cell performance.

Membrane Viscoelastic and Structural Properties. To assess the impact of the metal oxide–Nafion interfacial interaction on the bulk physical properties of the composite membrane, we carried out dynamic mechanical analysis (DMA) measurements on dried membrane samples. From the $\tan \delta$ variation of these measurements, we determined the glass-transition temperature of the membranes. In all cases, the glass-transition temperature (T_g) of the composite membranes is increased over a recast Nafion control. In addition, the increase in T_g correlates with the performance of the composite membranes in the PEMFCs operating above 100 °C. An increase in glass-transition temperature is indicative of a stiffening of the polymer system. This finding argues for a molecular-level interaction between the metal oxide surface and the polymer that effectively crosslinks the polymer strands, improving the mechanical rigidity of the system. The data also suggest that the glass-transition temperature of the membrane is a critical parameter in determining the high-temperature performance of a PEM fuel cell. It appears that once the glass transition occurs, the polymer system loses mechanical integrity and can no longer counterbalance the external stress applied by the fuel-cell frame or maintain the requisite hydration state, as both of these properties require a degree of polymer rigidity. Thus, it is critical that the membrane T_g be above the operating temperature of the fuel cell. All of the metal oxides tested show an increase in T_g ; however, because some of these materials do not lead to an improved high-temperature

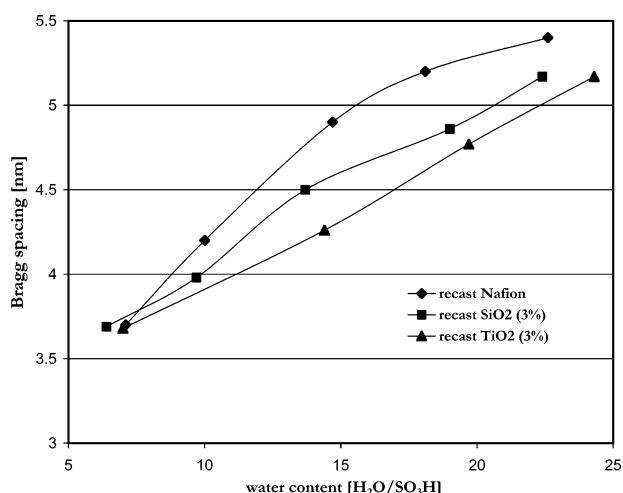


Figure 6. Small-angle X-ray studies of control recast Nafion, recast SiO₂, and recast TiO₂ composite membranes for various water contents. The reported Bragg spacing represents the average interionic cluster distance in the membranes.

membrane, the exact molecular details of the metal oxide–Nafion interfacial interaction appear to be a second critical parameter.

X-ray Diffraction Analysis. Small-angle X-ray scattering (SAXS) was utilized to investigate the structural changes in hydrated Nafion membranes¹² upon introduction of the inorganic phase. Recast Nafion, SiO₂ composite, and TiO₂ composite membranes were evaluated as a function of water content. Variation in the peak scattering angle was correlated with the Bragg spacing, which in turn represents the average interionic cluster distance.¹³ The Bragg spacing is reported to depend on the water content and equivalent weight of the membranes.¹⁴ From Figure 6, it can be seen that the Bragg spacing associated with metal-oxide-containing membranes shows closer ionic clusters than the unmodified Nafion membrane. It has been suggested that decreases in cluster-to-cluster distance correlate with cluster size, smaller separations being associated with larger cluster sizes.¹⁵ Therefore, hydrated silica- and titania-containing membranes support larger water clusters, consistent with the conclusion that these materials are mechanically stiffer at the molecular level. For the current data set, it can be seen that at hydration levels below ~ 7 waters/sulfonate group (relatively dehydrated), the Bragg spacing is invariant with metal oxide composition, further supporting the proposed relationship between water-cluster size and presence of the metal oxide phase. That is, below ~ 7 waters/sulfonate, the available water is a limiting reagent and improved structural membrane properties do not enhance the membrane aqueous phase. Once sufficient water is available, the ability of the Nafion phase to host larger water clusters with a closer contact becomes an enabling issue. The ability to support larger water clusters is likely

associated with the improved apparent cell conductivity under elevated temperature operational conditions in which the polymer is placed under significant external stress by the kinematics of the cell test frame.

Mechanism of Metal Oxide–Nafion Interactions. The data presented here argue strongly for a specific molecular interaction between the polymer matrix and the metal oxide particles. It is well-established that the surface hydroxyl groups¹⁶ on the metal oxide adsorb cations or anions from water and release protons or hydroxide ions into the solution. This behavior cannot be used to explain the observed cell response upon addition of a metal oxide phase, because Nafion, a perfluorosulfonic acid ionomer, is a strong acid and does not favor additional protons. In support of this statement, no significant change in proton concentration is observed by titration, as reported in Table 4, upon impregnation of the metal oxide particles. Potentially, three types of generic chemisorption sites are available on the metal oxide surface: a hydrogen-bonding site associated with a surface M–OH moiety, a ligation site associated with a coordinately unsaturated metal ion bonded to the oxygen of a SO₃[−] group, and a nonspecific physisorption site involving van der Waal interactions between the hydrophobic polymer backbone with the metal oxide surface.

To further probe the nature of the interfacial interaction, we undertook thermal gravimetric decomposition of recast Nafion and composite membranes with mass spectroscopic detection (TG-MS). A typical decomposition curve for a recast Nafion membrane that has not been exposed to liquid water is shown in Figure 7. The mass 18 trace indicates that two types of water are present in the film. The first loss of water occurs in a broad peak starting at 80 °C and maximizing at 150 °C. This signal is assigned to waters of hydration in the Nafion matrix. As can be seen from the mass-loss plot (Figure 9, bottom), these waters represent a small fraction of the native polymer mass. The second water-loss peak is observed to initiate at 280 °C and is concomitant with a mass 64 peak that is assigned to loss of SO₂. These two peaks align with the initiation of a major mass loss from the sample, indicative of Nafion thermal decomposition. The simultaneous loss of H₂O and SO₂ is assigned to the loss of sulfonic acid groups (SO₃H) from the polymer, as diagrammed in Figure 8. At temperatures ~ 400 °C, mass loss for the ether side chains (mass 47, COF⁺ fragment) and Teflonic polymer backbone (mass 131, C₃F₅⁺ fragment) are observed.

The TG-MS response changes dramatically upon addition of a TiO₂ component to the membrane, as shown in Figure 9. The most obvious change is a sharp mass loss at ~ 300 °C. Mass 18 and mass 46 signals mirror this change, showing sharp peaks centered at 300 °C that indicate the rapid loss of SO₃H groups. This contrasts sharply with the sulfonate loss peak of a pure Nafion membrane, which shows a large temperature spread for this decomposition (Figure 7 vs Figure 9). A small portion of the ether side chains is also observed to decompose at 300 °C in the case of the composite

(12) Deng, Q.; Cable, K. M.; Moore, R. B.; Mauritz, K. A. *J. Polym. Sci., Part B* **1996**, *34* (11), 1917–1923.

(13) Gierke, T. D.; Munn, G. E.; Wilson, F. C. *J. Polym. Sci., Part B* **1981**, *19* (11), 1687–1704.

(14) Manley, D. S.; Williamson, D. L.; Noble, R. D.; Koval, C. A. *Chem. Mater.* **1996**, *8* (11), 2595–2600.

(15) Elliott, J. A.; Hanna, S.; Elliott, A. M. S.; Cooley, G. E. *Polymer* **2001**, *42* (5), 2251–2253.

(16) Tamura, H.; Tanaka, A.; Mita, K.; Furuichi, R. *J. Colloid Interface Sci.* **1999**, *209* (1), 225–231.

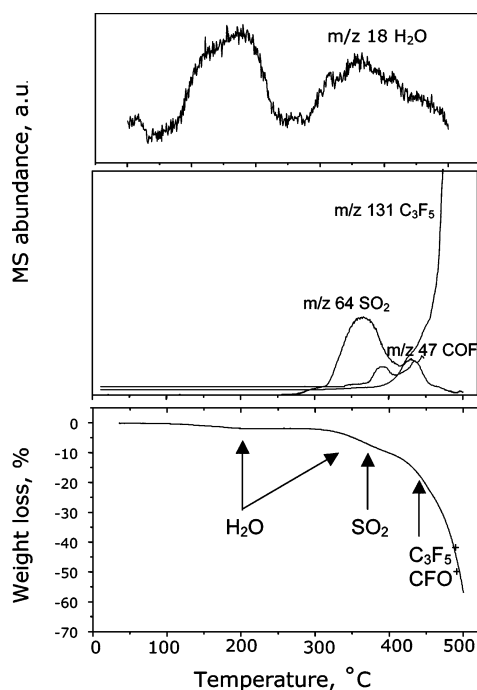


Figure 7. Thermal gravimetric mass spectroscopy (TGMS) of a (relatively) dry Nafion membrane. The bottom panel indicates the thermal gravimetric response of Nafion, showing total decomposition occurs above ~ 400 °C with minor events starting at ~ 300 °C. The top panel indicates the temperature-dependent appearance of an $m/z = 18$ amu species, which is assigned to water in the gas phase above the sample. Two peaks are observed. The lower-temperature peak is assigned to residual waters of hydration in the Nafion polymer. The higher-temperature peak is concomitant with the observation of an $m/z = 64$ amu peak (middle panel) assigned to SO_2 . These two signals taken together are a signature for the decomposition of the Nafion sulfonic acid moiety (SO_3H). The middle panel also reports on the temperature response of an $m/z = 47$ peak and an $m/z = 131$ peak, assigned to the Nafion side chain and Nafion backbone decompositions, respectively. The maximum in the mass spectral events are noted on the thermal curve in the bottom panel.

Thermal Decomposition of Nafion

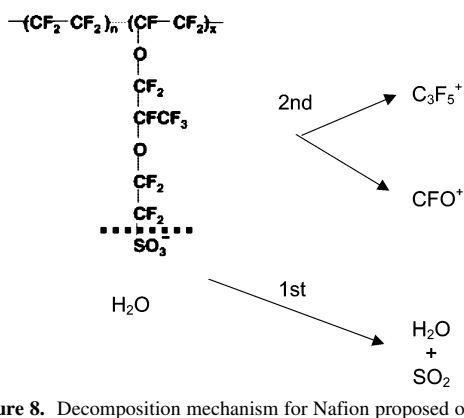


Figure 8. Decomposition mechanism for Nafion proposed on the basis of the data in Figure 7. The initial process involves loss of the sulfonic acid group from the polymer side chains, followed by decomposition of the side chains and the backbone.

membrane, although the bulk of the side chains and the polymer backbone are unaffected by the presence of titania. These data suggest that titania catalytically removes the Nafion sulfonate groups at 300 °C, a process that is possible only if there is a specific molecular contact between the

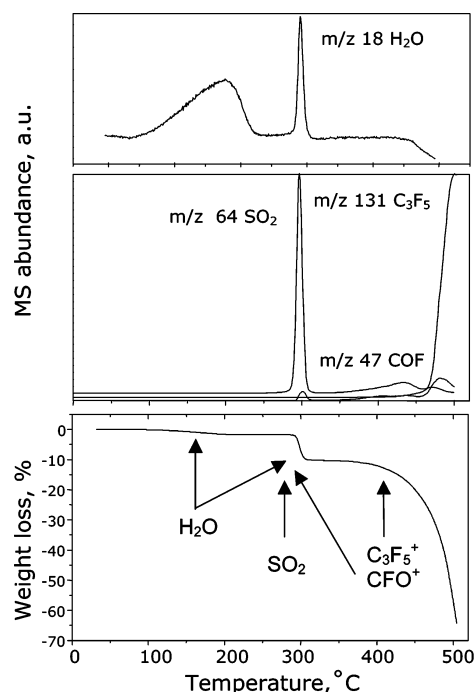


Figure 9. TGMS of a TiO_2 -Nafion composite membrane. Panels are arranged as noted in Figure 7. Notice that the main difference between the composite sample data shown here and that of the pure Nafion response in Figure 7 is a sharpening (and decreased temperature) of the $m/z = 18$ and 64 peaks associated with the cleavage of the SO_3H group. This change is specific for the catalytic decomposition of the sulfonate groups, indicating a direct molecular contact between the titania surface and this moiety.

sulfonate groups and the titania surface. Thus, a nonspecific interaction between the Nafion fluorocarbon backbone and the metal oxide surface is ruled out as the major interfacial interaction occurring in the composite. In addition, these data point to coordination bonding between the sulfonate group and a coordinately unsaturated Ti (IV) surface site as the most likely interfacial interaction as depicted in Figure 7b. Of the three molecular interactions postulated, only this one is expected to catalyze the loss of sulfonate groups from Nafion. This conclusion, along with the finding that a specific molecular interaction is critical to the enhanced thermal stability of composite fuel cell membranes, is further supported by the finding that both titania and silica additives introduce distinct (i.e., sharp) sulfonate loss peaks in the 300–400 °C range, whereas addition of either Al_2O_3 or ZrO_2 , materials that do not aid membrane performance, have very little impact on the membrane TG-MS traces of mass 18 and mass 46. Thus, a strong molecular interaction between sulfonate groups and the metal oxide surface correlates directly with an improved fuel-cell current–voltage response under elevated-temperature, low-humidity conditions.

Polymer–Metal Oxide Interactions: Structural Impacts. Data have been presented that indicate that Nafion in solution aggregates into rods, with the hydrophobic backbone making up the core of the rod and the hydrophilic sulfonate groups pointed toward the solvent, making rodlike fringes.¹⁷ The Nafion rods are generally several hundreds of nanometers in size, and no detectable Nafion ionomers are found in

(17) Jiang, S. H.; Xia, K. Q.; Xu, G. *Macromolecules* **2001**, *34* (22), 7783–7788.

Table 6. Glass-Transition Temperatures for Various Composite Membranes as Determined Using Dynamic Mechanical Analysis

| membrane material | glass-transition temperature, T_g (°C) |
|--|--|
| recast Nafion | 92 |
| Al ₂ O ₃ –Nafion | 95 |
| SiO ₂ –Nafion | 100 |
| ZrO ₂ –Nafion | 112 |
| TiO ₂ –Nafion | 120 |

solution. On the basis of this model of the Nafion solution, it is believed that the interaction of Nafion in solution with the various metal oxides plays a vital first step in making a successful elevated-temperature composite membrane. In the recasting process, the Nafion rods are expected to orient themselves around the metal oxide particles because of electrostatic and chemical interactions and, after evaporation of the solvent, form homogeneous composite membranes. If the Nafion–metal oxide interaction is too weak, the particles will precipitate out of solution and an inhomogeneous material will form. This latter condition is observed when large metal oxide particles are employed. Likewise, if the selected oxide interacts very weakly with the polymer surface, a homogeneous membrane will not form.

On the basis of the data presented here, it is postulated that the metal oxide particles act to crosslink the Nafion polymer chains. One consequence of this type of chemical interaction would be an increase in the glass-transition temperature (T_g)¹⁸ of the modified Nafion. This effect is observed using dynamic mechanical analysis (DMA), as reported in Table 6. Whereas the data in Table 6 provide a relative ordering of the glass-transition temperatures, the specific values measured do not necessarily reflect the glass-transition temperatures of membranes in the fuel-cell environment, because both the water content of the membrane and the external stress placed on the membrane by the fuel-cell test fixture will affect the glass-transition temperature. Nonetheless, it can be seen that the net effect of the inorganic phase is to shift the glassy phase transformation to higher temperatures.

This finding suggests that the loss of water observed at elevated cell temperatures may be caused by a change in polymer structure and not by direct evaporation of water from the electrolyte, as has previously been suggested. Consistent with this conclusion, it is noted that the loss in current–voltage response of recast Nafion-based cells with decreased humidity at elevated temperature (such as that shown in Figure 2) is irreversible. However, composite membranes containing a titania or silica phase produce a stable and significantly more reversible response with decreased humidity, as seen in Figure 3.

The lack of a direct impact on the properties of water by the inorganic phase is also supported by the observation that the addition of this phase changes neither the thermal gravimetric response of the membrane below ~200 °C, where water loss is expected to occur, nor the bulk hydrophobicity of the membrane, as measured by contact angle. Rather, the data presented here suggest that the

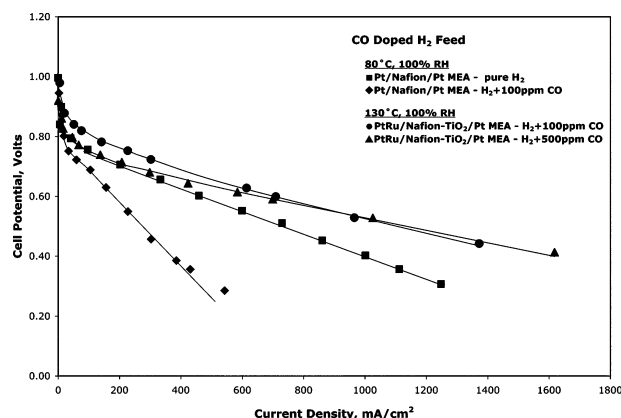


Figure 10. Current–voltage profiles showing the effect of cell temperature and electrode composition on carbon monoxide tolerance. In this data set, a cell (platinum anode) operating at 80 °C and exposed to 100 ppm of CO in the H₂ stream is compared with a pure hydrogen cell and elevated-temperature cells operating on 100 and 500 ppm carbon monoxide (with a PtRu anode).

elevation of the Nafion glass-transition temperature is the primary process that enables the composite material to be an effective fuel-cell membrane in the temperature range of interest. Given that freestanding Nafion membranes have a glass-transition temperature in the 90–110 °C range, as observed in the present study and reported elsewhere,¹⁹ elevation of this value (by ~20–30 °C) upon addition of an inorganic phase allows Nafion to maintain its self-assembled structure through the operating temperature range studied here (110–140 °C). The available data suggest that loss of water and thus membrane failure at elevated temperatures and low humidity is due to reorganization of the Nafion structure, either causing an expulsion of internal water or inducing discontinuities in the proton conductivity paths contained within Nafion below the glass-transition temperature.

It has been noted that the impregnation of the metal oxide does not help increase the membrane conductivity.²⁰ Conductivity measurements on freestanding membrane samples indicate that the composite membrane is slightly less conductive than a pure Nafion membrane, independent of humidity level. This finding is supportive of the crosslinking model proposed here. The effective crosslinking induced by the inorganic phase should somewhat decrease the proton conductivity of the membrane, as it both decreases the proton content of the membrane because of the sulfonate–metal oxide interactions (as observed by TG-MS and direct titration) and hinders the mobility of the sulfonate groups.

Carbon Monoxide Studies. Carbon monoxide studies were carried out using a hydrogen gas stream with 100 ppm CO to mimic the gas feed out of a fuel processor. Figure 10 shows the fuel-cell performance of a control Nafion at 80 °C without CO and with 100 ppm CO in the fuel stream and TiO₂ composite with 100 and 500 ppm CO in the fuel stream. A Pt–Ru anode electrocatalyst was used for the 500 ppm CO study. A precipitous drop in cell potential is

(18) Deng, Q.; Moore, R. B.; Mauritz, K. A. *J. Appl. Polym. Sci.* **1998**, *68* (5), 747–763.

(19) Yeo, S. C.; Eisenberg, A. *J. Appl. Polym. Sci.* **1977**, *21* (4), 875–898.

(20) Yang, C.; Srinivasan, S.; Bocarsly, A. B.; Tulyani, S.; Benziger, J. B. *J. Membr. Sci.* **2004**, *237*, (1–2), 145–161.

Table 7. Electrode Kinetic Parameters for Carbon Monoxide Studies with Recast Nafion and TiO₂ Composite Membranes

| membrane | <i>T</i> (°C) | RH (%) | <i>P</i> (atm) | CO concentration (ppm) | <i>E</i> ₀ (V) | <i>b</i> (mV/decade) | <i>R</i> (Ω cm ²) |
|-------------------------|---------------|--------|----------------|------------------------|---------------------------|----------------------|-------------------------------|
| control Nafion | 80 | 100 | 1 | no CO | 950 | 60 | 0.36 |
| | | | | 100 | 950 | 70 | 0.82 |
| TiO ₂ recast | 130 | 75 | 3 | 100 | 948 | 65 | 0.18 |
| | | | | 500 | 954 | 66 | 0.23 |

observed for control Nafion at 80 °C with 100 ppm CO. The performance of a TiO₂ composite with 100 ppm CO at 130 °C and 75% RH is also shown in Figure 11. For clarity purposes, the performance of control Nafion under these conditions is not included. The fuel-cell performance of control Nafion at 130 °C and 75% RH can be recalled from Figure 2. The high-temperature operation at 130 °C provided significant CO tolerance, and the incorporation of TiO₂ enabled low relative humidity operation. With the use of a Pt–Ru anode electrocatalyst, we minimized cell performance loss and it was possible to operate at 500 ppm CO. The electrode kinetic parameters for the CO studies are reported in Table 5. Note that the poisoned TiO₂ composite cell outperforms the 80 °C response of a Nafion membrane utilizing a pure H₂ fuel.

Summary

The method of preparing metal oxide composite Nafion membranes using solubilized Nafion and various metal oxide

particles produced a uniform, homogeneous distribution of metal oxide in the Nafion structure. Lower resistivities were attained at elevated temperatures and under reduced relative humidity operation in a PEMFC using titania and silica particles from either Alfa-Aesar or Degussa-Huls. The chemical interaction between the metal oxide surface and the Nafion membrane is vital for effective PEMFC performance. The titania and silica metal oxides from Degussa-Huls and the silica composite from Alfa-Aesar provided the best results at reduced relative humidity PEMFC operation.

Acknowledgment. The authors thank Dr. Jennifer Willson for her assistance in acquiring SEM images and Dr. Christopher Yang and Sonia Tulyani in acquiring the SAXS data. The authors also thank Global Photonics Energy Corporation for its financial assistance in this study. K.T.A. acknowledges the support of the United States Environmental Protection Agency Star Fellowship Program.

CM051781B